Interaction of protein SRP19 with signal recognition particle RNA lacking individual RNA-helices

Christian Zwieb
Department of Molecular Biology, The University of Texas Health Center at Tyler, PO Box 2003, Tyler, TX 75710, USA

Received February 21, 1991; Revised and Accepted May 8, 1991

ABSTRACT

Derivatives of human SRP-RNA were constructed by site-directed mutagenesis and tested for their ability to interact with protein SRP19. An RNA missing helix 6 barely interacts with SRP19, while the helix 8-deletion mutant retains much binding capability. A mutant RNA consisting just of helix 6 also binds the protein, but not as well as the unaltered molecule. SRP19 interacts to a full extent with the fourth mutant RNA composed of helices 6, 7, 8 and a portion of helix 5. It is concluded that helix 6—and not helix 8—is the major SRP19 binding site. Helices 7, 8 and portions of helix 5 contribute to the formation of a functional site. These results agree with data suggesting a proximity of helix 6 and the conserved part of SRP-RNA.

INTRODUCTION

The majority of secretory proteins require signal recognition particle (SRP) for translocation from the cytosol into the lumen of the endoplasmic reticulum (ER). SRP is part of the secretory apparatus which includes the signal peptide, ribosomes and the SRP-receptor in the ER-membrane (1, 2). SRP is a stable cytosolic ribonucleoprotein particle isolated and characterized particularly well from canine pancreas (3). It is composed of one RNA molecule (SRP-RNA) with 300 nucleotides and of six polypeptides (SRP9, SRP14, SRP19, SRP68, SRP72 and SRP54). The RNA consists of eight helices and shows some degree of tertiary structure (4, 5). It is contacted directly by all SRP-proteins, with the exception of SRP54. RNA-bound SRP19 is required for assembly of SRP54 (3, 6).

Mild digestion of the canine SRP with micrococcal nuclease generates two subparticles. SRP19 is present in the larger one, together with the conserved part of helix 5, helices 6–8, the SRP72/68 heterodimer and SRP54 (7). SRP19 protects the distal loops of helices 6 and 8 from digestion by α-sarcin (8). Recently, an octamer sequence near the C-terminus was shown to be required for interaction with SRP-RNA (9, 10).

To identify the determinants of SRP-RNA required for binding to SRP19 directly, individual helices were removed by site directed mutagenesis. RNAs were transcribed *in vitro* and tested for their ability to interact with SRP19. I demonstrate that the protein binds predominantly to helix 6. However, additional elements from the conserved portion of SRP-RNA are required to form a fully functional binding site.

MATERIAL AND METHODS

Construction of phR

Plasmid phR for synthesis of authentic human SRP-RNA was constructed by complete gene synthesis. Updated sequence information was obtained by analysis of plasmid 7L30.1 (11). The design of 16 oligonucleotides is shown in Figure 1a. 'Trityl on'-synthesis was accomplished on an Applied Biosystem DNA PCR-Mate using β-cyanoethyl-phosphoramidite chemistry. Oligonucleotides were purified and detritylated on purification cartridges supplied by the manufacturer and dissolved at a concentration of 8.5-nMol/ml. 2 μl of each oligonucleotide were added to a 1.5 ml Eppendorf tube in a total reaction of 50 μl containing 50 mM Tris-HCl pH 9.0, 100 mM MgCl, 50 mM DTT, 0.4 mM ATP and 10 units T4 polynucleotide kinase. Incubation was for 20 min at 37°C. 2 μl 250 mM EDTA (pH 8.0) and 348 μl of TE (10 mM Tris-HCl pH 7.5, 1 mM EDTA), 100 mM NaCl was added. The sample was heated for 5 min using a 300 ml beaker with boiling water. The beaker was placed at 4°C and left over night. The annealed DNA was extracted once with phenol and chloroform, adjusted to 300 mM NaCl and precipitated by adding 3 volumes of ethanol and incubation at −70°C for 1 hr. The assembled gene was recovered by centrifugation, washed once with 80% ethanol, dried and dissolved in 32 μl TE. Aliquots of the annealed oligonucleotides were ligated to about 100 ng of EcoRI- and BamHI-digested DNA of pUC18 for 3 hrs at room temperature and then placed at 4°C over night. The ligase was inactivated by a 10-min incubation at 70°C. The DNA was digested with KpnI for 20 min at 37°C to reduce the amount of circular pUC18 DNA. Competent *E. coli* DH5α cells (BRL) were transformed. Transformants were selected on LB plates containing 100 μg/ml ampicillin. DNA of individual transformants was prepared, restricted with EcoRI and BamHI and analyzed by agarose gel electrophoresis. A small number of clones containing inserted DNA was characterized by DNA sequencing with AMV reverse transcriptase (Stratagene) and α^{35}S-dATP using the 24-mer M13 reverse sequencing (−48) and the 17-mer M13 sequencing (−20) primers (New England Biolabs).

Construction of mutant plasmids

Mutants pΔH6, pΔH8 were constructed as described above for phR with a subset of the phR-oligonucleotides and additional mutant ones as indicated in Figure 1a. pH6 was assembled from four oligonucleotides as shown in Figure 1b. The Δ35-mutation

was obtained using the polymerase chain reaction (PCR) (12) with mutagenic oligonucleotide **b5** (ACTTAGTGCGGACAC-CCGATCTATAGTGCGTCGTATTAG) for the 5'- and **b3** (CAGGTCGACTCTAGAGGATCCACAGGCGCGATCCC-ACTAC) for the 3'-deletion. First, the 5'-deletion (pΔ5) was constructed with composite oligonucleotide **a** (TCCTGAAT-CTTCCCCTCCGTAGGCACCCCAGGCTTTACACT) and **b5**. The PCR product was used to synthesize mutant DNA by amplification with oligonucleotides **c** (TCCTGAATCTTCCCC-TCCGT) and **d** (CGCCAGGGTTTTCCCAGTCACGAC). Subsequently, the double deletion pΔ35 was obtained using pΔ5 DNA and mutagenic oligonucleotide **b3** with oligonucleotides **a**, **c** and **d**. The nature of all mutant plasmids was verified by DNA-sequencing.

Synthesis of SRP- and mutant RNAs

DNAs were digested with restriction enzymes DraI (phR, pΔH6 and pΔH8) or BamHI (pH6 and pΔ35), extracted with phenol and chloroform, concentrated by ethanol precipitation and dissolved in TE. RNA synthesis was initiated from the T7-promoter and carried out as described previously (9). For synthesis of radioactively labeled RNA, the concentration of UTP was reduced 50-fold and α^{32}P-UTP (ICN, 25 Ci/mmole) was added. Aliquots of the RNAs were analyzed by electrophoresis on 2% agarose and 6% polyacrylamide urea gels (13) and dissolved in water.

Binding of SRP19 and C-terminal deletion mutants

Binding of SRP19 and mutants to the various RNAs was monitored by retardation of SRP19::RNA complexes on DEAE-Sepharose. A 50-μl aliquot of the translation mix was adjusted to 300 mM KOAc; 1 μl water, 1 μg tRNA (*E. coli* $tRNA^{Phe}$, Boehringer) or 1 μg SRP-RNA transcribed from phR-wt (14). The sample was incubated 30 min. at 25°C, spun in an airfuge at 30 psi for 15 min. and the pellet (P) and a 5 μl aliquot of the supernatant (S) were dissolved in 50 μl SDS sample buffer. The main portion of the supernatant was loaded on an 80 μl DEAE-Sepharose column (Pharmacia) equilibrated with 300 mM KOAc, 100 mM Tris-HCl pH 7.5. The column was washed four times with 160 μl of 300 mM KOAc, 100 mM Tris-HCl pH 7.5 (flowthrough, F) and four times with 160 μl of 2 M KOAc, 100 mM Tris-HCl pH 7.5 (eluate, E). 70 μl TCA was added to the pooled fractions and samples were kept on ice for 30 min.. Polypeptides were pelleted by a 10-min. centrifugation, supernatants were removed, and pellets were dissolved in 100 μl SDS sample buffer. SDS polyacrylamide gel electrophoresis of aliquots of the samples was carried out as described above. After staining and destaining, gels were dried and exposed to X-ray film. Individual bands were quantitated using exposure times in the linear response range of a Abaton 300/GS scanner.

SRP19 deletions were obtained by translation of run-off transcripts generated by digestion of plasmids pΔC1 and pΔC2 with HindIII. Immunoprecipitation was carried out as described (9). The stability of RNAs in the binding assay was confirmed by adding uniformly ^{32}P-labeled transcripts to the wheat germ lysate and incubation at 25°C for 0, 10 and 30 min. Samples were extracted with phenol and chloroform, precipitated with ethanol and analyzed by electrophoresis on 6% polyacrylamide urea gels.

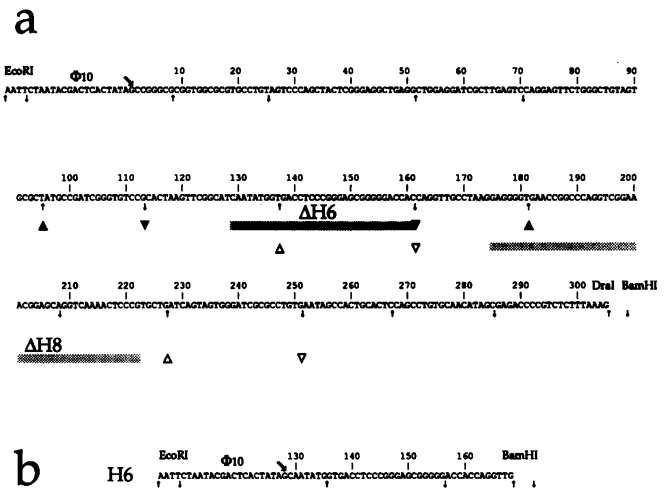

Figure 1. Construction of phR for synthesis of authentic human SRP-RNA and mutant derivatives ΔH6, ΔH8 (**a**) and H6 (**b**). Sequences of human SRP-RNA and mutant H6 are shown between EcoRI and BamHI restriction sites. T7-polymerase promoters (Φ10) and the guanosines at the start of transcription (→) are indicated. Transcripts are numbered on top of the sequences. The borders between the synthetic oligonucleotides identical to the shown sequence are marked by arrows pointing up. Borders of oligonucleotides with complementary sequences are marked with arrows pointing down. Likewise, borders between oligonucleotides used for construction of mutants are indicated by solid (ΔH6) or open triangles (ΔH8). Deleted regions are emphasized with a dark gray (ΔH6) and a light gray horizontal bar (ΔH8).

RESULTS

Construction of plasmids and analysis of RNAs

phR, a plasmid for transcription of authentic human SRP-RNA by T7-polymerase, was assembled by complete gene synthesis (14). Sequences of the annealed 16 overlapping synthetic oligonucleotides are indicated in Figure 1a. The number of transformants containing only pUC18 was reduced by digestion of the ligation mixture with KpnI. About 10% of the clones harbored stable inserts and about half of those contained the proper sequence. Human SRP-RNA was obtained by restricting phR with DraI and transcription by T7-polymerase as described in Material and Methods. Absorbance measurement at 260 nm and quantitation of ethidium bromide stained RNA after gel electrophoresis showed that 100 to 150 molecules of RNA were obtained from one plasmid molecule (not shown). Electrophoretic mobilities of *in vitro* transcribed SRP-RNA and of SRP-RNA isolated from canine SRP were identical (Figure 3a). Both RNAs bound efficiently to SRP19 (15, 9).

To construct mutants pΔH6 and pΔH8, a subset of the phR-oligonucleotides was used together with overlapping mutant oligonucleotides (Figure 1a). Mutations for the removal of individual SRP-RNA helices were chosen on the basis of secondary structure information obtained by comparative sequence analysis (4). Helix 6 was removed in ΔH6; helix 8 was lacking in ΔH8. Their postulated secondary structures are shown in Figure 2. Stable RNAs of the expected sizes were obtained after restriction of mutant DNAs with DraI and transcription with T7-polymerase (Figure 3). pH6 was assembled from four oligonucleotides (Figure 1b). To construct pΔ35, PCR-technology was used (12) with the oligonucleotides described in Material and Methods. The

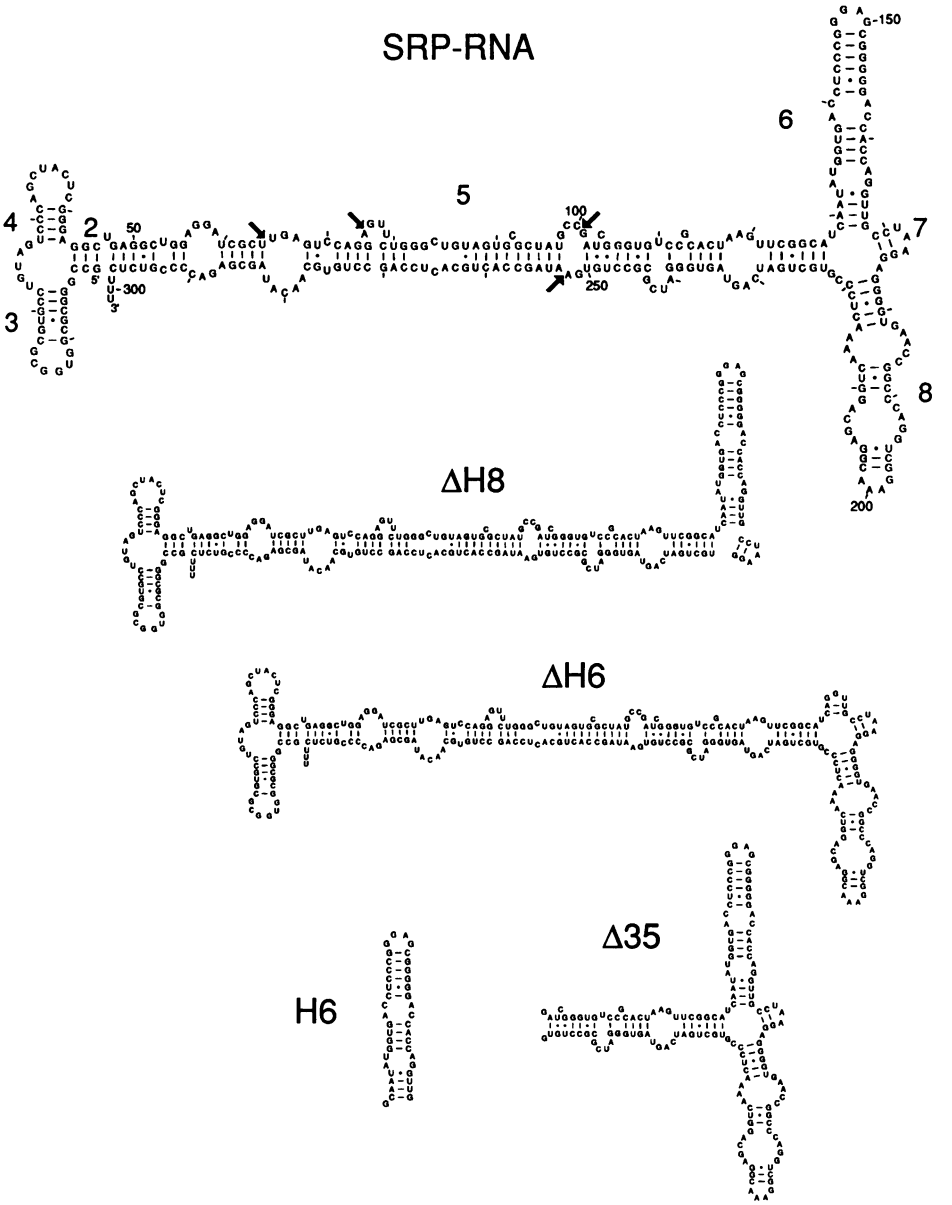

Figure 2. Secondary structures of human SRP-RNA and ΔH6, ΔH8, H6 and Δ35. The secondary structure of human SRP-RNA is shown on top with large numbers 2 to 8 for the seven helices (4). Arrows indicate hypersensitive cutting sites for micrococcal nuclease (7).

latter method was less time consuming and more efficient than complete gene synthesis. The corresponding RNAs (H6 and Δ35) were obtained after restriction of plasmid DNAs with BamHI and run-off transcription (Figures 3).

The stability of SRP-RNA and mutant transcripts under the conditions of the binding assay was determined. RNAs were labeled radioactively with α^{32}P-UTP during transcription. Results shown in Figure 3b demonstrate that the integrity of the RNAs was not affected by incubation in the wheat germ cell-free system.

Binding of SRP19 to SRP-RNA and mutant RNAs

Binding of human SRP19 to human SRP-RNA or mutant RNAs was monitored by retardation of SRP19::RNA complexes on DEAE-Sepharose as described previously (9). Polypeptides were analyzed by SDS gel electrophoresis and autoradiography. SRP19 was translated and labeled in the wheat germ cell-free system in the presence of ^{35}S-methionine and allowed to form a complex with the various RNAs. At 300 mM potassium acetate, RNA-bound SRP19 was retarded on DEAE, from which it was eluted with 2 M potassium acetate. Figure 4 shows that—in the presence of SRP-RNA—most of SRP19 was recovered in the high salt eluate. In the absence of SRP-RNA, virtually all the protein bound to the ribosomal pellet or the flowthrough of the DEAE-colum (Figure 4).

Binding of SRP19 to ΔH6 was greatly reduced, while ΔH8 bound SRP19 efficiently, albeit not as well as the unmutated SRP-RNA. H6 also bound SRP19, yet with some reduced efficiency.

The reduced amounts found in the eluates of the mutants are predominantly due to the appearance of SRP19 in the flowthrough and not in the pellets. An appreciable amount of the protein was found in the ribosomal pellet only in ΔH6 (Figure 4). The results were confirmed by titration experiments with variable amounts of added SRP- or mutant RNAs (Figure 4); they demonstrate that helix 6 is the major binding site of SRP19. Using mutant Δ35, I tested if binding to SRP19 could be improved by a contribution of helices 5, 7 and 8. Titration with SRP-RNA and Δ35 showed that binding was completely restored (Figure 5).

Binding of C-terminal deletion mutants of SRP19 to mutant RNAs

The C-terminus of SRP19 is lysine-rich in lysines and could interact with SRP-RNA. Although it was shown that removal of up to 24 amino acids retains binding (9, 10), a secondary role of the lysine-rich C-terminus in interaction with SRP-RNA was not excluded. Since the binding site of SRP19 appeared to be complex, the possibility was considered that the C-terminus might selectively interact with helix 6 or helix 8, or portions common to ΔH6, ΔH8 and Δ35. Binding of SRP-RNA, ΔH6, ΔH8 and H6 to proteins SRP19, ΔC1 (14 amino acids deleted) and ΔC2 (24 amino acids deleted) was tested. The results shown in Figure 6 demonstrate that the protein deletions bound to all SRP-RNA derivatives. No significant differences in the affinity to the various RNA mutants were detected.

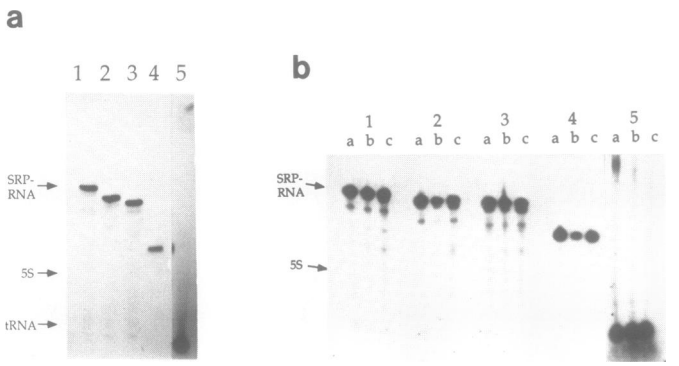

Figure 3. Autoradiogram of transcribed SRP-RNA and mutant derivatives (**a**). Stability of the RNAs in the wheat germ cell-free system (**b**). RNAs were labeled and transcribed and separated on 6% polyacrylamide gels containing 7 M urea. Lanes 1: SRP-RNA, lanes 2: ΔH6, lanes 3: ΔH8, lanes 4: Δ35, lanes 5: H6. Positions of canine SRP-RNA, 5S RNA and tRNA are marked by arrows. RNAs were incubated for 0 (lanes a), 10 (lanes b) or 30 min (lanes c) under protein binding conditions. Because helix 6 is short and GC-rich, it was labeled poorly with α^{32}P-UTP; to visualize, this part of the gel was exposed longer.

DISCUSSION

Characterization of mutant RNAs

Mutant plasmids were constructed by complete gene synthesis or recombinant PCR using structural information derived by comparative sequence analysis (4). Helix 6 was explicitly removed in ΔH6 and was synthesized as a separate molecule (mutant H6). Helix 6 is specific for the eucaryotes and archaea, but deleted in the bacterial 4.5S RNA and the 6S scRNA of *Bacillus subtilis* (16). Although helix 6 sequences are variable, the secondary structures are highly conserved. The stem is likely to be continuously stacked and the four partly conserved purines in the terminal loop might be in the so-called tetra-loop structure (17). This loop was protected by SRP19 in footprinting experiments (8). Four purines are located also in the terminal loop of helix 8 and are protected by SRP19. In contrast to helix 6, helix 8 is highly conserved and present in all SRP-RNA including the bacterial 4.5S RNAs (4).

Mutant Δ35 contains the most conserved part of the SRP-RNA plus variable helix 6 (Figure 2). The termini of Δ35 were chosen to coincide with two hypersensitive micrococcal nuclease cutting sites. Digestion with micrococcal nuclease was used previously to separate SRP in two structurally and functionally distinct domains (7). It was anticipated that Δ35 would be able to adapt a structure similar to the one present in the larger of the two SRP domains.

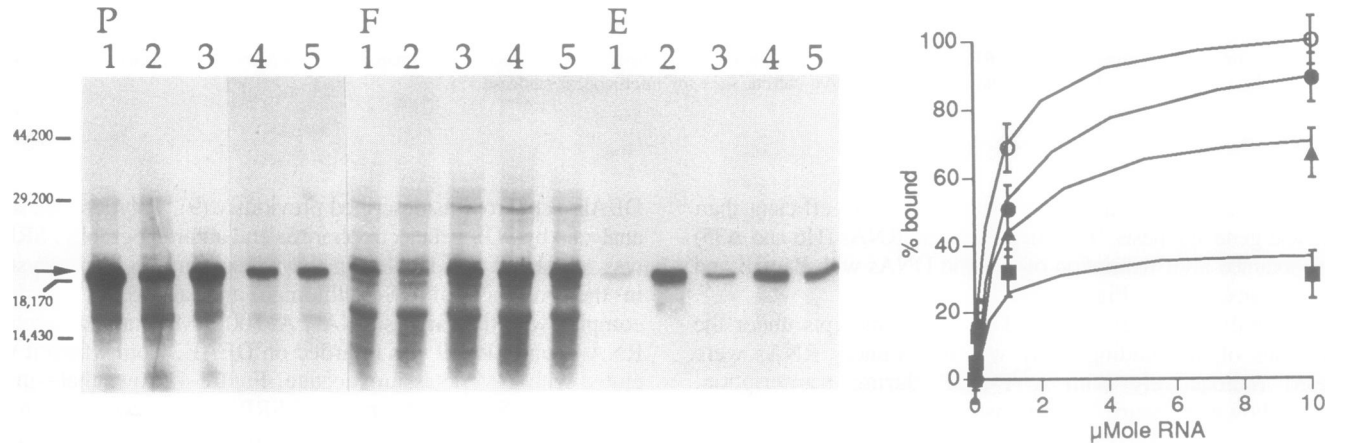

Figure 4. Affinity of protein SRP19 to SRP-RNA and ΔH6, ΔH8 and H6. Complexes were analyzed by retardation on DEAE-Sepharose. Polypeptides from equal aliquots of the ribosomal pellet (P), the flowthrough (F) and the high-salt eluate (E) were separated on SDS polyacrylamide gels and exposed to X-Ray film. Lanes 1: no RNA, lanes 2: SRP-RNA, lanes 3: ΔH6, lanes 4: ΔH8, lanes 5: H6. The positions of SRP19 (arrow) and molecular weight markers are shown in each panel. Results shown in the autoradiogram are from the addition of 1 μMole of RNA to a 50 μl binding reaction. Titration of RNAs is displayed in the graph on the right. Data were obtained using different exposure times in the linear response range of an Abaton 300/GS scanner. SRP-RNA (○), ΔH6 (■), ΔH8 (●), H6 (▲). The extent of binding is expressed as the percentage of SRP19 bound to 10 μMole of unmutated SRP-RNA.

SRP-RNA and mutant derivatives were obtained by run-off transcription with T7-polymerase toward DraI- or BamHI-sites. Transcripts from phR yielded SRP-RNA with three uridine bases at the 3'-end corresponding in size to canine SRP-RNA. Because of a known property of the polymerase, it cannot be excluded that one or two nucleotides were added to the 3'-end. Intact molecules of the expected size were obtained in all cases. RNAs were unaffected by a 30-min incubation in the wheat germ cell-free system under protein binding conditions. The overall structure of SRP- and mutants RNA appears to be similar (Figure 2) since comparable minor degradation products were observed after gel electrophoresis (Figure 3) on overexposed autoradiograms (not shown). Δ35 yielded the most stable RNA, which is consistent with its expected high degree of folding.

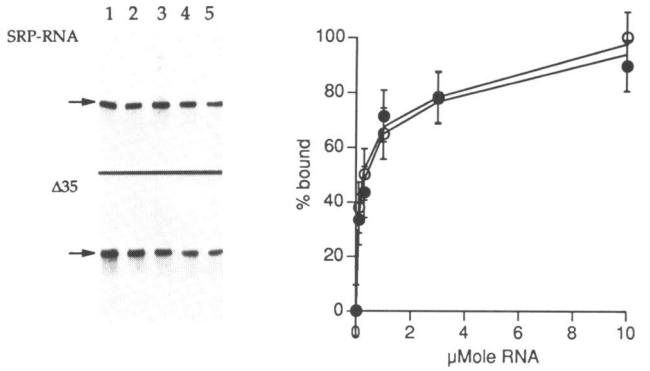

Figure 5. Affinity of protein SRP19 to SRP-RNA (●) and Δ35 (○). Autoradiogram of the SDS polyacrylamide gel is showing the polypeptides recovered in the high salt eluates: lane 1: 0.1, lane 2: 0.3, lane 3: 1.0, lane 4: 3.0, lane 5: 10 μMole added RNA. The positions of SRP19 is indicated by the arrows. Titration of RNAs is displayed in the graph on the right. The extent of binding is expressed as the percentage of SRP19 bound to 10 μMole of unmutated SRP-RNA.

Characteristics of the SRP19 binding site

Binding of human SRP19 to human SRP-RNA and the four mutant RNAs was monitored by retardation of SRP19::RNA complexes on DEAE-Sepharose. ΔH6 interacted poorly with SRP19; ΔH8 and H6 bound efficiently, albeit not as well as the unmutated SRP-RNA; Δ35 completely restored binding. Minor amounts of material present in the eluate without added SRP-RNA were probably due to the presence of wheat germ SRP-RNA in the lysate (18).

The results demonstrate that the binding site of SRP19 is complex, with the predominant binding site located in helix 6. SRP19 interacts probably with the four partly conserved purines (GGAG) of the distal loop (4, 8), yet other nucleotides might be involved as well. It seems likely that formation of a stem is required to expose the bases in the loop in the proper conformation—possibly a tetra-loop (17). The weak binding of SRP19 to ΔH6 could be explained by the fact that a very similar tetra-loop sequence (GAAA) occurs in helix 8. It remains to be determined, if this minor interaction is indeed part of the binding site. Protection of the distal loop of helix 8 from α-sarcin digestion could be explained by shielding, and not direct binding. The conclusion that helix 6 is the predominant binding site is consistent with the recent finding that SRP19 is unable to interact with *E.coli* 4.5S RNA (19).

Seven of the nine amino acids at the C-terminus of SRP19 are lysines. The lysine-rich tail has been suggested to be involved in interaction with SRP-RNA (15). Analysis of C-terminal deletion mutants of SRP19 showed 24 C-terminal amino acids to be dispensable (9, 10). When the RNA-mutants were tested for interaction with the C-terminal mutants ΔC1 and ΔC2, no significant differential effect was detected, making it even less

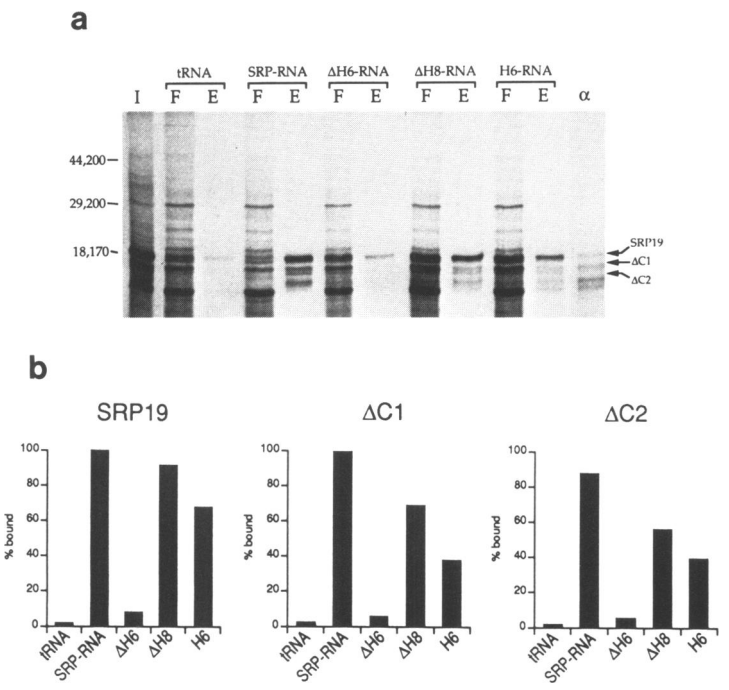

Figure 6. Affinity of protein SRP19 and C-terminal deletions to SRP-RNA and mutant derivatives ΔH6, ΔH8 and H6. A mixture of SRP19, ΔC1 and ΔC2 polypeptides was analyzed by retardation on DEAE-Sepharose. Equal aliquots of the input before fractionation (I), the flowthrough (F) and the eluate (E) were analyzed by SDS gel electrophoresis after incubation with tRNA, SRP-RNA, ΔH6, ΔH8 or H6 (**a**). Immunoprecipitated polypeptides are seen in lane α. Positions of SRP19, ΔC1 and ΔC2 (arrows) and molecular weight markers are indicated. Autoradiograms from various exposure times were scanned and data were plotted as shown in (**b**).

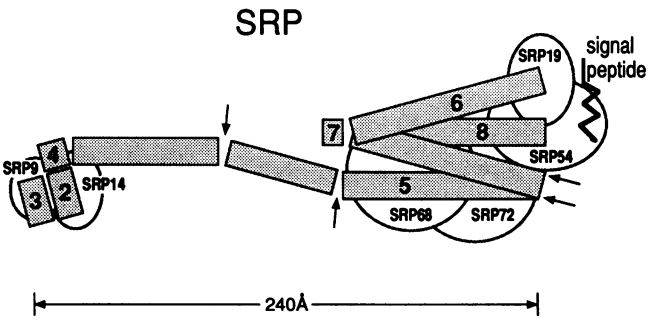

Figure 7. Map of SRP. Helices are represented as rectangles and are numbered from 2 to 8 as in Figure 2. SRP-proteins are sketched as ovals; their sizes are approximated assuming globular structure (24). The signal peptide is shown to interact directly with SRP54 (25). Micrococcal nuclease hypersensitive sites (7) are marked by arrows. Folding is proposed to occurs at two hypersensitive sites. SRP19 is positioned at the distal loops of helices 6 and 8 (8) and SRP54. The length of SRP (240 Å), as determined in the electron microscope (22) is indicated at the bottom. Other features are shown for which there is some evidence (4, 21), but which are not discussed in the context of this work.

probable that the lysine-rich tail functions in interaction with SRP-RNA.

As shown in Figure 5, the full binding capacity was restored with Δ35. This result supports the concept that—besides helix 6—the conserved portion of SRP-RNA is important for binding. Under the assumption that SRP19 is a globular protein, the distal loops of helix 6 and 8 must be close to each other to be both protected, which could be accomplished by folding of the RNA in the vicinity of SRP19. This view is confirmed by comparative sequence analysis (4) and molecular modeling (20, 21) studies aimed to accommodate the RNA within the dimensions of SRP determined by electron microscopy. A hypothetical folding design is shown in a map of SRP (Figure 7). To bring the distal loops of helices 6 and 8 closer, helices 5, 6 and 8 were positioned parallel to each other by folding the RNA at two of the sites that are hypersensitive toward micrococcal nuclease digestion. Physical model building of the RNA shows that as a consequence of such folding, its size and shape agrees well with the dimensions (240×60 Å) determined in the electron microscope (22). Only SRP-RNA and mutant Δ35 restore complete binding, presumably because they conform to the suggested folding pattern. Binding of SRP19 could not be improved using a mixture of equimolar amounts of ΔH6 and H6 (not shown) indicating that helix 6 must be placed properly in the context of nucleotides located in the proximal parts of helices 6, 7 and 8. This region has been found to contain dynamic properties (23) which were proposed to play a role in assembling the particle (5). It is possible—as was suggested recently (10)-that SRP19 directly affects the formation of an RNA structure needed for further assembly of SRP.

ACKNOWLEDGEMENT

This work was supported by a Biomedical Research Support Grant, identification number 2-S07-RR-05958-04.

REFERENCES

1. Walter P. and Lingappa V. (1986) Ann. Rev. Cell Biol. **2**, 499–516
2. Rapoport T.A. (1990) TIBS **15**, 355–358
3. Walter P. and Blobel G. (1983) Cell **34**, 525–533
4. Larsen N. and Zwieb C. (1991) Nucleic Acids Res. **19**, 209–215
5. Zwieb C. (1989) in: Prog. in Nucleic Acid Res. and Mol. Biol. **37**, 207–234
6. Siegel V. and Walter P. (1988) Cell **52**, 39–49
7. Gundelfinger E.D., Krause E., Melli M. and Dobberstein B. (1983) Nucleic Acids Res. **11**, 7363–7374
8. Siegel V. and Walter P. (1988) Proc. Natl. Acad. Sci. U.S.A. **85**, 1801–1805
9. Zwieb C., submitted
10. Römisch K., Webb J., Lingelbach K., Gausepohl H. and Dobberstein B. (1990) J. Cell Biol. **111**, 1793–1802
11. Ullu E. and Weiner A.M. (1984) EMBO J. **3**, 3303–3310
12. Nelson R.M. and Long G.L. (1989) Anal. Biochem. **180**, 147–151
13. Maniatis T., Fritsch E. and Sambrook J. (1982) in: Molecular Cloning, A Laboratory Manual, Cold Spring Harbor Laboratory
14. Romaniuk, P.J., deStevenson, I.L. and Wong, H.-H. A. (1987) Nucleic Acids Res. **15**, 2737–2755
15. Lingelbach K., Zwieb C., Webb J.R., Marshallsay C., Hoben P.J., Walter P., and Dobberstein B. (1988) Nucleic Acids Res. **16**, 9431–9442
16. Toschka H.Y., Struck J.C.R. and Erdmann V.A. (1989) Nucleic Acids Res. **17**, 31–36
17. Cheong C., Varani G. and Tinoco I. Jr. (1990) Nature (London) **346**, 680–682
18. Prehn S., Wiedmann M., Rapoport T.A., and Zwieb C. (1987) EMBO J. **6**, 2093–2097
19. Ribes V., Römisch K., Giner A., Dobberstein B. and Tollervey D. (1990) Cell **63**, 591–600
20. Zwieb C., and Schüler D. (1989) Biochem. and Cell Biol. **67**, 434–442
21. Zwieb C., unpublished
22. Andrews D., Walter P. and Ottensmeyer P. (1987) EMBO J. **6**, 3471–3477
23. Zwieb C. and Ullu, E. (1986) Nucleic Acids Res. **14**, 4639–4657
24. Zwieb C. (1986) Endocyt. C. Res. **3**, 41–51
25. Kurzchalia T., Wiedmann M., Girshovich A., Bochkareva E., Bielka H. and Rapoport T. (1986) Nature **320**, 634–636